

(Interscience, New York, 1962).

²³F. W. J. Oliver, in *Handbook of Mathematical Functions*, edited by M. Abramowitz and I. A. Stegun, Natl. Bur. Std. (U.S. GPO, Washington, D.C., 1964), p. 379.

²⁴G. G. Emch and G. L. Sewell, *J. Math. Phys.* **9**, 946 (1968).

²⁵R. Kubo, *J. Phys. Soc. Jap.* **17**, 1100 (1962); in *Fluctuations, Relaxation, and Resonance in Magnetic Systems*, edited by D. ter Haar (Oliver and Boyd, Edinburgh, 1962), p. 23.

²⁶G. S. Agarwal, *Phys. Rev.* **178**, 2025 (1969).

²⁷G. S. Agarwal and E. Wolf, *Phys. Rev. Lett.* **21**, 180 (1968).

²⁸G. S. Agarwal, *Phys. Rev.* **177**, 400 (1969).

²⁹J. H. Marburger and W. H. Louisell, *Phys. Rev.* **186**, 174 (1969).

³⁰U. Fano, *Rev. Mod. Phys.* **29**, 74 (1957).

³¹R. M. Wilcox, *J. Math. Phys.* **8**, 962 (1967).

³²E. W. Smith, C. R. Vidal, and J. Cooper, *J. Res. Natl. Bur. Stand. (U.S.)* **73A**, 405 (1969).

³³J. Cooper, *Rev. Mod. Phys.* **39**, 167 (1967).

Structure Factor and Radial Distribution Function for Liquid Argon at 85°K[†]

J. L. Yarnell, M. J. Katz, and R. G. Wenzel

Los Alamos Scientific Laboratory, University of California, Los Alamos, New Mexico 87544

S. H. Koenig

IBM Thomas J. Watson Research Center, Yorktown Heights, New York 10598

(Received 29 January 1973)

The structure factor $S(Q)$ for liquid argon at 85°K has been determined in a neutron scattering experiment to an accuracy of ≈ 0.01 . The problem of obtaining $S(Q)$ from the results of neutron scattering measurements, made as a function of scattering angle using a detector with an energy-dependent efficiency, is considered in detail. Smooth curves for $S(Q)$ and its Fourier transform, the radial distribution function $g(r)$, were obtained from the experimental data by an iterative procedure suggested by Verlet and carried out by Schiff, and are tabulated for convenience. The experimental results are in excellent agreement with the predictions of computer simulations based on either the Lennard-Jones two-body interaction, or on the Barker, Fisher, and Watts potential with corrections for three-body and quantum effects included.

I. INTRODUCTION

This paper reports highly accurate results for the structure factor $S(Q)$ of liquid argon near its triple point, as obtained from measurements of the angular dependence of the scattering of slow monochromatic neutrons by a sample of ^{36}Ar . To obtain these results, it was necessary to combine good counting statistics with careful attention to the various corrections which must be applied to the experimental data.

Much information about the equilibrium properties of a liquid can be obtained from $S(Q)$. In addition, one may compare the experimentally determined $S(Q)$ with $S(Q)$ deduced from computer simulations based on classical mechanics and an assumed interparticle interaction. Ideally, one may also obtain the interparticle pair potential $\varphi(r)$ from $S(Q)$ using classical theories of monatomic fluids.

When the present experiment was undertaken it was becoming clear that no existing neutron or x-ray scattering data were of sufficient accuracy to allow a reliable interaction potential to be deduced from the data, even assuming that the theories were exact and applicable at the experimental fluid

densities. Levesque and Verlet^{1,2} had argued that even the then current, extensive x-ray scattering data of Mikolaj and Pings³ for argon near the critical point were inadequate; they showed that structure factor data of less than 1% uncertainty are required to obtain $\varphi(r)$ with a precision of 10%. It is now generally appreciated that (particularly at liquid densities) the general form of $S(Q)$ is determined by geometric effects due to the short-range repulsive core of $\varphi(r)$. It is only the secondary features of $S(Q)$ that are influenced by the form of $\varphi(r)$ external to this hard core.

The present experiment was an attempt to obtain $S(Q)$ with an uncertainty of the order of 0.01. Neutron scattering was used in preference to x-ray scattering, since neutron scattering is by the atomic nucleus and is isotropic for slow neutrons, thereby eliminating (uncertain) corrections for the atomic form factor. Additionally, sample cells can be built of materials which make corrections for background scattering simpler for the case of neutron scattering. Liquid argon near the triple point was chosen because its thermodynamics are well understood, $\varphi(r)$ is reasonably well known, the atomic density is high, and there is an isotope (^{36}Ar) with a very large scattering cross section

(78 b)⁴ that is 100% coherent.

To obtain $S(Q)$ from the raw data requires corrections for a multitude of effects, all of which are examined in some detail in Appendixes A, B, and C. The methods used are extensions of those proposed by North, Enderby, and Egelstaff.⁵ In brief, the procedure consists of three steps: (1) calibration of the apparatus using an incoherent scatterer of known cross section, (2) determination of $S(Q)$ on an absolute basis using the best available estimates of the cross sections and corrections involved, and (3) refinement of the corrections by requiring that $S(Q)$ and its Fourier transform $g(r)$ (the radial distribution function) take on the correct limiting values as their arguments approach zero.

For some purposes, smooth curves for $S(Q)$ and $g(r)$ are desired. Such curves were obtained by an iterative procedure suggested by Verlet and carried out by Schiff.⁶ The results so obtained for $S(Q)$ and $g(r)$ are listed in Tables I and II, respectively.

The fully corrected $S(Q)$ is in excellent agreement with the predictions of molecular-dynamics calculations⁷ using the Lennard-Jones 6:12 potential for argon, and systematically deviates from computations in which a hard-sphere interaction is assumed for $\varphi(r)$. The liquid structure predicted by molecular dynamics using the Lennard-Jones potential is essentially the same as that obtained from Monte Carlo calculations⁸ based on the very accurate potential derived by Barker, Fisher, and Watts,⁹ and which include three-body interactions and quantum effects. At the present level of accuracy, the results of the two computer simulations are in equally good agreement with the data.

II. THEORETICAL BACKGROUND

The intensity of the radiation scattered coherently by a monatomic isotropic fluid of N atoms will differ from that scattered incoherently by N atoms because of interference among the waves scattered from different atoms. For an idealized experiment—one in which a beam of incident neutrons is scattered through an angle 2θ by atoms considered to be fixed in their instantaneous positions during the scattering (so that the scattering is elastic)—the interference effects are obtained by summing the scattered amplitudes over all N atoms, which takes into account phase shifts due to differences in path lengths, and then squaring and averaging over all thermal equilibrium configurations of the system. This gives the angular-dependent structure factor

$$S(Q) = \frac{1}{N} \left\langle \left| \sum_{j=1}^N e^{i\vec{Q} \cdot \vec{r}_j} \right|^2 \right\rangle_{av} \quad (1)$$

where the \vec{r}_j are the positions of the atoms. \vec{Q}

$= \vec{k}_0 - \vec{k}$ is the change in de Broglie wave vector of the neutrons of incident momentum $\hbar\vec{k}_0$, and is related to the scattering angle by $Q = 2k_0 \sin\theta$. This is the formal definition of $S(Q)$. Expanding the summation in Eq. (1) gives

$$S(Q) = \frac{1}{N} \left\langle N + \sum_{i \neq j} \sum e^{i\vec{Q} \cdot (\vec{r}_i - \vec{r}_j)} \right\rangle_{av}. \quad (2)$$

If the pair-distribution function $g(r)$ is defined such that

$$n(r) dr = 4\pi n_0 g(r) r^2 dr \quad (3)$$

is the average number of atoms in a spherical shell of thickness dr and radius r centered about an atom known to be at $r=0$, where n_0 is the average number density of atoms, then in the limit $N \rightarrow \infty$, Eq. (2) becomes

$$S(Q) = 1 + n_0 \int_V g(r) e^{i\vec{Q} \cdot \vec{r}} d\vec{r} \quad (4)$$

$$= 1 + n_0 \int_V [g(r) - 1] e^{i\vec{Q} \cdot \vec{r}} d\vec{r} + n_0 \delta(Q). \quad (5)$$

The integration is over the volume of the fluid. The δ function represents the coherent forward scattering [the only contribution to $S(Q)$ of a structureless liquid]; it is negligible in practice at scattering angles greater than $\sim 10^{-2}$ seconds of arc, and customarily dropped from the definition of $S(Q)$, Eq. (5). Then $S(Q) - 1$ and $g(r) - 1$ become a Fourier-transform pair, and after performing the angular integrations (the fluid is regarded as isotropic), are related by

$$S(Q) - 1 = (4\pi n_0 / Q) \int_0^\infty [g(r) - 1] r \sin(Qr) dr, \quad (6)$$

$$g(r) - 1 = (2\pi^2 n_0 r)^{-1} \int_0^\infty [S(Q) - 1] Q \sin(Qr) dQ. \quad (7)$$

The limiting values of $S(Q)$ and $g(r)$ as their arguments approach zero give integral relationships which $S(Q)$ must satisfy, and which are used in refining the calculated corrections to the data (see below). From Eq. (5) one obtains

$$S(0) = 1 + 4\pi n_0 \int_V [g(r) - 1] d\vec{r}, \quad (8)$$

which from the compressibility equation¹⁰ reduces to

$$S(0) = k_B T n_0 \chi_T, \quad (9)$$

where k_B is Boltzmann's constant, T is the absolute temperature, and χ_T is the isothermal compressibility of the fluid. Because of the strong interatomic repulsion at short range, $g(0)=0$, and Eq. (7) gives

$$2\pi^2 n_0 = - \int_0^\infty Q^2 [S(Q) - 1] dQ. \quad (10)$$

One of the main problems in the theory of classical fluids has been to derive $S(Q)$ and $g(r)$ from $\varphi(r)$. It then becomes straightforward to calculate the thermodynamic properties of the fluid. The

experimental problem, on the other hand, has been to measure $S(Q)$ in order to derive information about $\varphi(r)$. To a first approximation the naive experiment, in which the normalized angular dependence of the scattered intensity from a beam of monochromatic incident neutrons is measured, gives $S(Q)$ directly. To obtain $S(Q)$ accurately, however, corrections of two classes are necessary: those due to the fact that the experiment does not, in principle, measure $S(Q)$, except approximately, and those due to the usual experimental limitations. The former are discussed in detail in Appendix A. The latter are considered in Appendix B. Suffice it to say here (cf. Van Hove¹¹) that the differential cross section for scattering into an element of solid angle $d\Omega$ about the scattered neutron direction, with spread $d\omega$ about an energy change ω (in units of \hbar), is

$$\frac{d^2\sigma_{coh}}{d\Omega d\omega} = b_{coh}^2(k/k_0)S(Q, \omega), \quad (11)$$

where b_{coh} is the bound-atom coherent scattering length, and $S(Q, \omega)$ is the generalized Van Hove response function¹¹ related to $S(Q)$ by

$$S(Q) = \int_{-\infty}^{\infty} S(Q, \omega) d\omega \quad (12)$$

with Q held constant in the integration.

Experimentally, a detector with an energy-dependent efficiency $\epsilon(k)$ is used to count neutrons scattered at a preset scattering angle θ , so that an effective integrated cross section is measured:

$$\left(\frac{d\sigma_{coh}}{d\Omega} \right)_{eff} = b_{coh}^2 \int_{-\infty}^{\omega_{max}} \epsilon(k) \left(\frac{k}{k_0} \right) S(Q, \omega) d\omega \quad (13)$$

with θ constant, and $\omega_{max} = E_0$. The problem is to relate this measured quantity to the liquid structure factor $S(Q)$. For neutrons, which have a non-negligible mass m compared to the mass M of argon atoms, the departure of k/k_0 from unity, the variation of $\epsilon(k)$, and the differences between constant θ and constant Q integration give rise to corrections of the order m/M at large scattering angles. These corrections are of critical importance in determining $S(Q)$ to an accuracy of 0.01.

III. APPARATUS AND PROCEDURES

The measurements were carried out on a neutron-diffraction spectrometer located at the Los Alamos Omega West Reactor. The reactor was operated at a power of 8 MW. Reflection from the (220) planes of a copper single crystal was used to select a monochromatic beam of neutrons from the reactor spectrum. The incident neutron beam was monitored by a ^{235}U fission counter, and the scattered neutrons were detected by a $^{10}\text{BF}_3$ proportional counter with a ceramic end window. The spectrometer collimation was chosen to provide a resolution in 2θ of $0.5^\circ - 0.7^\circ$ full width at

half-maximum over the angular range used in the experiment.

The cryostat used to contain the liquid ^{36}Ar sample is shown in Fig. 1. To avoid diffraction peaks in the background, the cell containing the ^{36}Ar sample was made of a Ti-Zr null matrix alloy.¹² The thickness of the argon sample was 0.105 cm, while the combined thickness of the two walls of the sample holder was 0.078 cm. The sample cell was surrounded by helium gas at a pressure equal to the internal pressure in the cell to avoid distortion of the flat walls of the cell and to promote thermal equilibrium. The temperature of the sample was maintained at 85.0 ± 0.2 °K by thermal contact with a reservoir of liquid argon of normal isotopic composition. The sample was condensed from a gas which contained 0.6% N_2 , 0.06% ^{36}Ar , 0.03% ^{40}Ar , and the remainder ^{36}Ar . The amount of liquid condensed into the cell was such as to produce a liquid-vapor interface near the top of the cell, ensuring that the liquid was in equilibrium with vapor

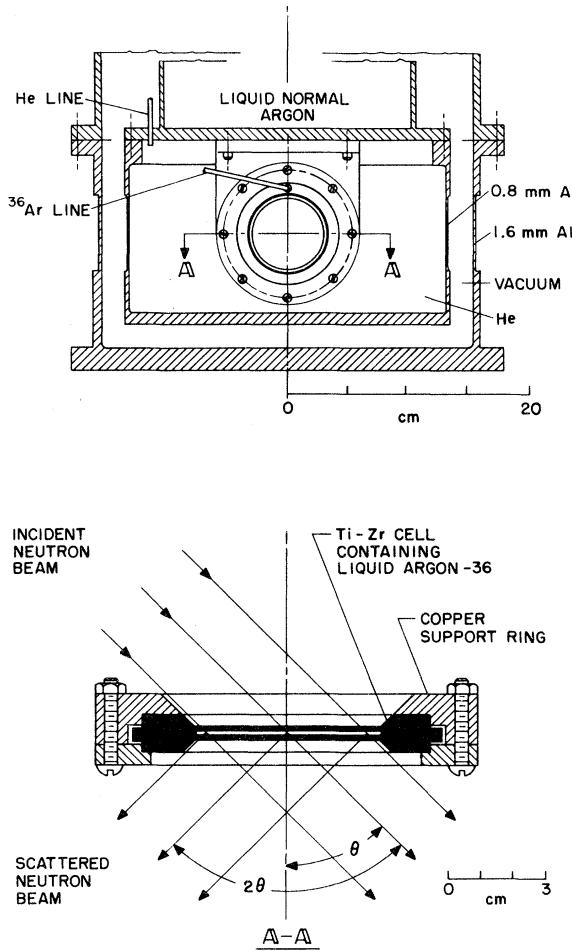


FIG. 1. Cryostat and cell used to contain the liquid- ^{36}Ar sample.

at the temperature of the cell.

The incident neutron beam was masked so that its projection on the cell fell within the uniform central portion of the cell at all scattering angles. The spectrometer was programmed to maintain the normal to the cell at $\frac{1}{2}$ the scattering angle, as shown in Fig. 1. The sample cell could be replaced by a vanadium disk of the same external dimensions for purposes of calibration. The width of the spectrometer resolution function was determined from the known collimator geometry and the mosaic properties of the monochromator crystal, and was checked against the measured widths of the Bragg peaks of a standard powder sample. The agreement was excellent.

In a typical experimental run counts were taken at 0.1° intervals for 2θ between 3.2° and 90.0° . At each angle scattered neutrons were counted until 75 000 monitor counts had been accumulated. All final results are based on the average of a number of such runs.

The neutron transmission at 0° scattering angle was measured for the vanadium standard, the empty Ti-Zr cell, and the ^{36}Ar sample. The transmissions, which are used in the data analysis, were found to be 0.864 ± 0.004 for the standard, 0.927 ± 0.006 for the cell, and 0.854 ± 0.004 for the sample. In the latter case, care was taken to measure the transmission over a region known to be completely filled with liquid.

The sample thickness, as indicated by its transmission, was somewhat greater than that typically used by other workers. This choice leads to improved statistical accuracy, at the cost of increasing the fraction of the incident neutrons which are multiply scattered. It is shown in the Appendixes that, for the geometry of the present experiment, the multiply scattered component is almost independent of the scattering angle and can be subtracted accurately, even for the relatively thick sample which we used.

IV. EXPERIMENTAL RESULTS

The raw data, counts vs θ (half the scattering angle), are shown in Fig. 2. The upper points are the average of 9 runs with the cell plus argon, and the lower points are the average of 11 runs with the empty cell. The intrinsic resolution of the apparatus at three scattering angles is also indicated in Fig. 2.

The incident neutron wavelength was determined to be $0.97819 \pm 0.00008 \text{ \AA}$ from an analysis of the Bragg peaks of the powder pattern of a standard (NbO) sample, for which accurate spacings have recently been determined by x rays.¹³ At 85°K the liquid in equilibrium with its vapor has an atomic density¹⁴ of 0.02125 \AA^{-3} (this is the value for ^{40}Ar and, assuming no quantum corrections, is the

same for ^{36}Ar).

The corrections required to transform the effective single scattering cross section per argon atom into $S(Q)$ are discussed in Appendix A. They are referred to collectively as Placzek¹⁵ corrections, and result from the fact that the atoms of the liquid move during the scattering, due both to their thermal motion and to recoil.

To obtain the effective cross section for single scattering, a series of corrections must be made to the raw data: resolution, background, transmission, effective sample volume, spectrometer efficiency, multiple scattering, and second-order contamination of the incident beam. These corrections are discussed in Appendix B and, when combined with the Placzek corrections, yield $S(Q)$ on an absolute basis to the accuracy with which the corrections of Appendix B can be made.

The experimental absolute values of $S(Q)$ may be further refined by imposing the restrictions Eqs. (9) and (10), which the correct $S(Q)$ must satisfy. These refinements are discussed in Appendix C. Figure 3 shows the experimental results for $S(Q)$ after all corrections and refinements have been applied.

The standard deviation of the individual data points due to counting statistics is nearly independent of Q . Its average value over the range of Q used in the present experiment is calculated to be 0.017. In Appendix A the maximum error in the Placzek corrections as we have used them is estimated to be of the order of 0.002. We believe that the Q dependence of the other corrections has been determined to a similar level of accuracy. We estimate that the over-all systematic error in the refined experimental values of $S(Q)$ is less than 0.01 for all values of Q .

For many purposes it is desirable to extend the experimental $S(Q)$ to a wider range of Q than that for which measurements were made, and to represent the experimental data by a smooth curve. This may be accomplished by an iterative procedure suggested by Verlet.⁸ It is based on the requirements that a physically meaningful $g(r)$ cannot contain oscillations of wavelength small compared to an atomic diameter and that, because of the strong repulsion which prevents atomic overlap, $g(r)$ must vanish for all r appreciably smaller than an atomic diameter. The procedure also yields a smooth curve for $g(r)$, and provides a check on the internal consistency of the experimental $S(Q)$.

Verlet's procedure, as applied to the present experimental data by Schiff,⁶ consists of the following steps:

(1) The experimental $S(Q)$ is extended in a reasonable way to values of Q beyond the range of measurement, in both directions. In the present instance the results of a molecular-dynamics cal-

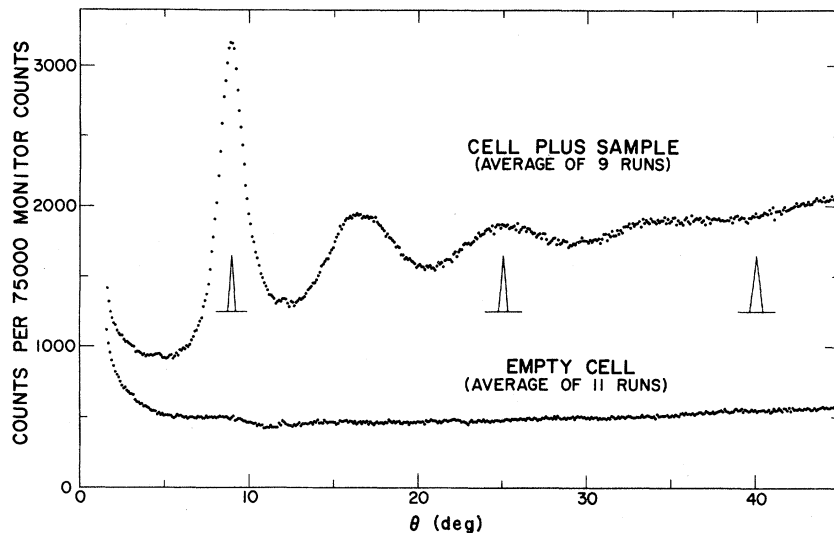


FIG. 2. Raw experimental data for neutrons scattered through an angle 2θ by the cell plus the ^{36}Ar sample and by the empty cell. The instrumental resolution is indicated at three scattering angles.

culation⁷ were used as a guide in extending the experimental data to large Q . The low- Q data were extended smoothly to the compressibility limit, Eq. (9), at $Q=0$. However, the initial choice of the way in which the data are extended affects only the rapidity of convergence and not the final result.

(2) The trial $S(Q)$ so obtained is Fourier transformed to obtain a provisional $g(r)$.

(3) The provisional $g(r)$ is modified by setting $g(r)=0$ for r out to approximately 0.8 of an atomic diameter, and by smoothing out any hump or dip appearing on a large scale drawing of $g(r)$.

(4) The modified $g(r)$ is transformed back to $S(Q)$.

(5) The resulting $S(Q)$ is smoothed to suppress any remaining short-wavelength wiggles. If there

are no systematic errors in the corrected data, the procedure will converge after a few iterations to yield a smoothed and extended $S(Q)$ which agrees with the experimental data over the range of Q for which data exist, and which transforms to a $g(r)$ which is smooth and close to zero for small r . On the other hand, for some data with significant systematic distortions, the procedure is known not to converge.⁸ Since the procedure combines the neutron scattering data with all other available information concerning $S(Q)$, it gives the best experimental determination of $S(Q)$ that can be obtained.

The smoothed and extended $S(Q)$ obtained by Schiff after one iteration of the above procedure is shown as a solid line in Fig. 3 and is listed in Table I. Its Fourier transform is shown in Fig. 4

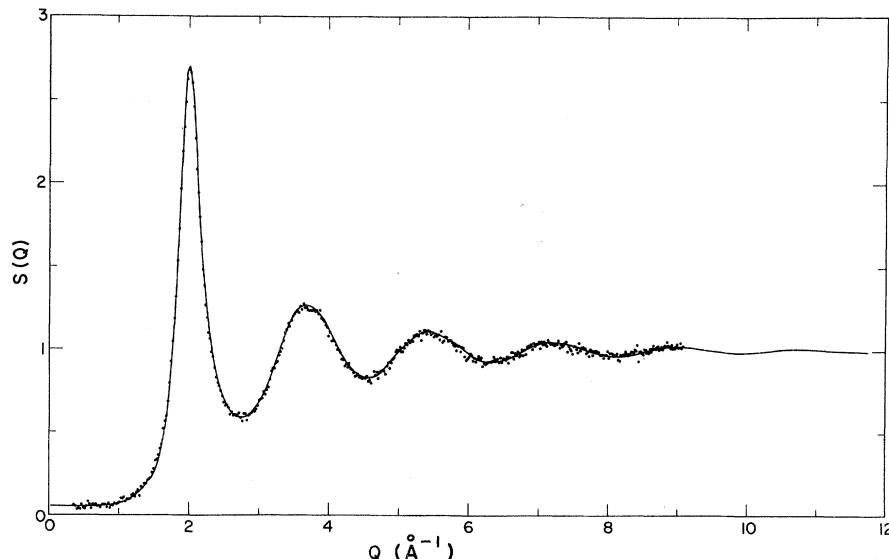


FIG. 3. Fully corrected experimental values of the liquid structure factor $S(Q)$ for ^{36}Ar at 85 °K. The solid line is a smoothed and extended $S(Q)$ obtained from the experimental data by an iterative procedure described in the text. The small dip in the experimental data near the top of the second peak ($Q = 3.75 \text{\AA}^{-1}$) is apparently statistical in origin.

TABLE I. Smoothed and extended $S(Q)$ for liquid argon at 85 °K obtained from the experimental data by the iterative procedure described in the text. The units for Q are \AA^{-1} .

Q	S(Q)	Q	S(Q)								
.0294	.0522	1.9971	2.7013	3.9648	1.1486	5.9325	1.0013	7.9001	.9782	9.8678	.9839
.0587	.0519	2.0264	2.6329	3.9941	1.1253	5.9618	.9912	7.9295	.9757	9.8972	.9840
.0881	.0516	2.0558	2.4791	4.0235	1.1012	5.9912	.9811	7.9589	.9734	9.9266	.9842
.1175	.0513	2.0852	2.2698	4.0529	1.0768	6.0206	.9711	7.9883	.9714	9.9559	.9845
.1468	.0510	2.1145	2.0386	4.0822	1.0523	6.0499	.9618	8.0176	.9697	9.9853	.9851
.1762	.0508	2.1439	1.8142	4.1116	1.0280	6.0793	.9535	8.0470	.9681	10.0147	.9858
.2056	.0507	2.1733	1.6149	4.1410	1.0040	6.1087	.9465	8.0764	.9668	10.0441	.9868
.2349	.0504	2.2026	1.4475	4.1703	.9807	6.1380	.9409	8.1057	.9656	10.0734	.9878
.2643	.0502	2.2320	1.3095	4.1997	.9586	6.1674	.9366	8.1351	.9648	10.1028	.9890
.2937	.0501	2.2614	1.1941	4.2291	.9383	6.1968	.9334	8.1645	.9644	10.1322	.9902
.3231	.0500	2.2907	1.0944	4.2584	.9201	6.2261	.9310	8.1938	.9646	10.1615	.9913
.3524	.0500	2.3201	1.0061	4.2878	.9042	6.2555	.9293	8.2232	.9654	10.1909	.9925
.3818	.0500	2.3495	.9283	4.3172	.8903	6.2849	.9283	8.2526	.9667	10.2203	.9936
.4112	.0500	2.3789	.8619	4.3465	.8780	6.3142	.9280	8.2819	.9685	10.2496	.9949
.4405	.0500	2.4082	.8076	4.3759	.8670	6.3436	.9284	8.3113	.9706	10.2790	.9963
.4699	.0500	2.4376	.7645	4.4053	.8571	6.3730	.9296	8.3407	.9731	10.3084	.9977
.4993	.0500	2.4670	.7302	4.4347	.8485	6.4023	.9312	8.3700	.9759	10.3377	.9992
.5286	.0500	2.4963	.7015	4.4640	.8415	6.4317	.9334	8.3994	.9791	10.3671	1.0007
.5580	.0500	2.5257	.6759	4.4934	.8363	6.4611	.9359	8.4288	.9824	10.3965	1.0020
.5874	.0500	2.5551	.6525	4.5228	.8331	6.4905	.9389	8.4581	.9859	10.4258	1.0033
.6167	.0500	2.5844	.6317	4.5521	.8316	6.5198	.9423	8.4875	.9894	10.4552	1.0045
.6461	.0510	2.6138	.6149	4.5815	.8319	6.5492	.9464	8.5169	.9928	10.4846	1.0056
.6755	.0540	2.6432	.6029	4.6109	.8338	6.5786	.9511	8.5463	.9960	10.5140	1.0067
.7048	.0550	2.6725	.5957	4.6402	.8373	6.6079	.9565	8.5756	.9990	10.5433	1.0076
.7342	.0560	2.7019	.5923	4.6696	.8429	6.6373	.9623	8.6050	1.0018	10.5727	1.0084
.7636	.0580	2.7313	.5914	4.6990	.8505	6.6667	.9684	8.6344	1.0047	10.6021	1.0090
.7930	.0590	2.7606	.5921	4.7283	.8603	6.6960	.9747	8.6637	1.0075	10.6314	1.0093
.8223	.0600	2.7900	.5944	4.7577	.8721	6.7254	.9810	8.6931	1.0102	10.6608	1.0096
.8517	.0610	2.8194	.5989	4.7871	.8852	6.7548	.9874	8.7225	1.0128	10.6902	1.0097
.8811	.0620	2.8488	.6066	4.8164	.8992	6.7841	.9939	8.7518	1.0153	10.7195	1.0097
.9104	.0630	2.8781	.6179	4.8458	.9136	6.8135	1.0005	8.7812	1.0175	10.7489	1.0097
.9398	.0640	2.9075	.6326	4.8752	.9282	6.8429	1.0071	8.8106	1.0194	10.7783	1.0096
.9692	.0660	2.9369	.6499	4.9046	.9429	6.8722	1.0135	8.8399	1.0211	10.8076	1.0094
.9985	.0680	2.9662	.6688	4.9339	.9575	6.9016	1.0196	8.8693	1.0226	10.8370	1.0090
1.0279	.0730	2.9956	.6889	4.9633	.9721	6.9310	1.0250	8.8987	1.0238	10.8664	1.0085
1.0573	.0780	3.0250	.7102	4.9927	.9863	6.9604	1.0299	8.9280	1.0247	10.8957	1.0079
1.0866	.0830	3.0543	.7335	5.0220	1.0000	6.9897	1.0342	8.9574	1.0252	10.9251	1.0072
1.1160	.0890	3.0837	.7594	5.0514	1.0127	7.0191	1.0380	8.9868	1.0252	10.9545	1.0065
1.1454	.0950	3.1131	.7882	5.0808	1.0246	7.0485	1.0413	9.0162	1.0247	10.9838	1.0058
1.1747	.1050	3.1424	.8196	5.1101	1.0356	7.0778	1.0440	9.0455	1.0239	11.0132	1.0052
1.2041	.1140	3.1718	.8529	5.1395	1.0462	7.1072	1.0461	9.0749	1.0228	11.0426	1.0045
1.2335	.1240	3.2012	.8871	5.1689	1.0565	7.1366	1.0474	9.1043	1.0216	11.0720	1.0038
1.2628	.1350	3.2305	.9218	5.1982	1.0665	7.1659	1.0481	9.1336	1.0202	11.1013	1.0031
1.2922	.1440	3.2599	.9569	5.2276	1.0762	7.1953	1.0483	9.1630	1.0187	11.1307	1.0025
1.3216	.1570	3.2893	.9927	5.2570	1.0852	7.2247	1.0479	9.1924	1.0171	11.1601	1.0019
1.3510	.1700	3.3186	1.0292	5.2863	1.0929	7.2540	1.0473	9.2217	1.0154	11.1894	1.0015
1.3803	.1900	3.3480	1.0660	5.3157	1.0992	7.2834	1.0464	9.2511	1.0136	11.2188	1.0010
1.4097	.2045	3.3774	1.1020	5.3451	1.1038	7.3128	1.0452	9.2805	1.0117	11.2482	1.0007
1.4391	.2179	3.4068	1.1360	5.3744	1.1069	7.3421	1.0437	9.3098	1.0098	11.2775	1.0002
1.4684	.2345	3.4361	1.1667	5.4038	1.1085	7.3715	1.0417	9.3392	1.0080	11.3069	.9998
1.4978	.2562	3.4655	1.1932	5.4332	1.1086	7.4009	1.0392	9.3686	1.0063	11.3363	.9992
1.5272	.2854	3.4949	1.2153	5.4626	1.1073	7.4302	1.0363	9.3979	1.0046	11.3656	.9986
1.5565	.3245	3.5242	1.2334	5.4919	1.1046	7.4596	1.0331	9.4273	1.0029	11.3950	.9979
1.5859	.3749	3.5536	1.2478	5.5213	1.1005	7.4890	1.0296	9.4567	1.0012	11.4244	.9972
1.6153	.4363	3.5830	1.2589	5.5507	1.0953	7.5184	1.0260	9.4860	.9994	11.4537	.9965
1.6446	.5085	3.6123	1.2665	5.5800	1.0894	7.5477	1.0223	9.5154	.9976	11.4831	.9959
1.6740	.5925	3.6417	1.2705	5.6094	1.0832	7.5771	1.0183	9.5448	.9959	11.5125	.9952
1.7034	.6927	3.6711	1.2708	5.6388	1.0770	7.6065	1.0142	9.5742	.9943	11.5419	.9945
1.7327	.8175	3.7004	1.2676	5.6681	1.0711	7.6358	1.0099	9.6035	.9929	11.5712	.9939
1.7621	.9775	3.7298	1.2615	5.6975	1.0654	7.6652	1.0055	9.6329	.9914	11.6006	.9935
1.7915	1.1818	3.7592	1.2535	5.7269	1.0595	7.6946	1.0014	9.6623	.9901	11.6300	.9933
1.8209	1.4321	3.7885	1.2440	5.7562	1.0531	7.7239	.9974	9.6916	.9887	11.6593	.9932
1.8502	1.7189	3.8179	1.2332	5.7856	1.0461	7.7533	.9938	9.7210	.9874	11.6887	.9934
1.8796	2.0196	3.8473	1.2209	5.8150	1.0382	7.7827	.9904	9.7504	.9862	11.7181	.9937
1.9090	2.3011	3.8767	1.2066	5.8443	1.0297	7.8120	.9872	9.7797	.9852	11.7474	.9941
1.9383	2.5270	3.9060	1.1897	5.8737	1.0207	7.8414	.9840	9.8091	.9845		
1.9677	2.6663	3.9354	1.1703	5.9031	1.0112	7.8708	.9811	9.8385	.9841		

TABLE II. Radial distribution function $g(r)$ for liquid argon at 85 °K obtained by Fourier transforming the smoothed and extended $S(Q)$ listed in Table I. The units for r are Å.

r	$g(r)$	r	$g(r)$	r	$g(r)$	r	$g(r)$	r	$g(r)$	r	$g(r)$
.0681	.0789	4.6308	.7730	9.1935	.9431	13.7562	1.0259	18.3189	.9880	22.8816	1.0038
.1362	.0545	4.6989	.7219	9.2616	.9587	13.8243	1.0232	18.3870	.9883	22.9497	1.0040
.2043	.0263	4.7670	.6862	9.3297	.9757	13.8924	1.0201	18.4551	.9890	23.0178	1.0039
.2724	.0062	4.8351	.6571	9.3978	.9943	13.9605	1.0163	18.5232	.9902	23.0859	1.0036
.3405	.0008	4.9032	.6293	9.4659	1.0138	14.0286	1.0120	18.5913	.9918	23.1540	1.0032
.4086	.0088	4.9713	.6023	9.5340	1.0326	14.0967	1.0074	18.6594	.9934	23.2221	1.0028
.4767	.0222	5.0394	.5796	9.6021	1.0492	14.1648	1.0030	18.7275	.9948	23.2902	1.0025
.5448	.0313	5.1075	.5651	9.6702	1.0628	14.2329	.9992	18.7956	.9960	23.3583	1.0024
.6129	.0305	5.1756	.5604	9.7383	1.0738	14.3010	.9958	18.8637	.9970	23.4264	1.0022
.6810	.0206	5.2437	.5640	9.8064	1.0830	14.3691	.9924	18.9318	.9981	23.4945	1.0020
.7491	.0082	5.3118	.5725	9.8745	1.0913	14.4372	.9886	18.9999	.9995	23.5626	1.0016
.8172	.0010	5.3799	.5829	9.9426	1.0988	14.5053	.9843	19.0680	1.0011	23.6307	1.0010
.8853	.0031	5.4480	.5945	10.0107	1.1048	14.5734	.9798	19.1361	1.0027	23.6988	1.0003
.9534	.0123	5.5161	.6091	10.0788	1.1082	14.6415	.9758	19.2042	1.0043	23.7669	.9998
1.0215	.0222	5.5842	.6294	10.1469	1.1079	14.7096	.9730	19.2723	1.0054	23.8350	.9995
1.0896	.0259	5.6523	.6569	10.2150	1.1041	14.7777	.9715	19.3404	1.0062	23.9031	.9994
1.1577	.0203	5.7204	.6911	10.2831	1.0977	14.8458	.9713	19.4085	1.0066	23.9712	.9993
1.2258	.0085	5.7885	.7291	10.3512	1.0904	14.9139	.9719	19.4766	1.0071	24.0393	.9991
1.2939	.0026	5.8566	.7675	10.4193	.0835	14.9820	.9727	19.5447	1.0076	24.1074	.9988
1.3620	.0065	5.9247	.8043	10.4874	1.0774	15.0501	.9734	19.6128	1.0082	24.1755	.9984
1.4301	.0011	5.9928	.8395	10.5555	1.0716	15.1182	.9740	19.6809	1.0088	24.2436	.9980
1.4982	.0095	6.0609	.8751	10.6236	1.0648	15.1863	.9748	19.7490	1.0091	24.3117	.9977
1.5663	.0180	6.1290	.9137	10.6917	1.0559	15.2544	.9763	19.8171	1.0090	24.3798	.9977
1.6344	.0180	6.1971	.9569	10.7598	1.0448	15.3225	.9786	19.8852	1.0085	24.4479	.9978
1.7025	.0086	6.2652	1.0038	10.8279	1.0322	15.3906	.9816	19.9533	1.0077	24.5160	.9980
1.7706	.0053	6.3333	1.0520	10.8960	1.0196	15.4587	.9847	20.0214	1.0070	24.5841	.9981
1.8387	.0155	6.4014	1.0983	10.9641	1.0083	15.5268	.9878	20.0895	1.0064	24.6522	.9981
1.9068	.0157	6.4695	1.1398	11.0322	.9986	15.5949	.9905	20.1576	1.0059	24.7203	.9980
1.9749	.0058	6.5376	1.1753	11.1003	.9901	15.6630	.9929	20.2257	1.0054	24.7884	.9979
2.0430	.0076	6.6057	1.2048	11.1684	.9818	15.7311	.9954	20.2938	1.0048	24.8565	.9980
2.1111	.0153	6.6738	1.2287	11.2365	.9727	15.7992	.9983	20.3619	1.0038	24.9246	.9983
2.1792	.0111	6.7419	1.2475	11.3046	.9628	15.8673	1.0015	20.4300	1.0026	24.9927	.9987
2.2473	.0038	6.8100	1.2608	11.3727	.9527	15.9354	1.0050	20.4981	1.0013	25.0608	.9991
2.3154	.0210	6.8781	1.2685	11.4408	.9438	16.0035	1.0084	20.5662	1.0001	25.1289	.9994
2.3835	.0295	6.9462	1.2706	11.5089	.9375	16.0716	1.0112	20.6343	.9992	25.1970	.9996
2.4516	.0232	7.0143	1.2679	11.5770	.9342	16.1397	1.0135	20.7024	.9986	25.2651	.9996
2.5197	.0052	7.0824	1.2618	11.6451	.9335	16.2078	1.0152	20.7705	.9980	25.3332	.9997
2.5878	.0128	7.1505	1.2536	11.7132	.9347	16.2759	1.0167	20.8386	.9974	25.4013	.9998
2.6559	.0176	7.2186	1.2435	11.7813	.9364	16.3440	1.0180	20.9067	.9966	25.4694	1.0002
2.7240	.0030	7.2867	1.2304	11.8494	.9381	16.4121	1.0191	20.9748	.9957	25.5375	1.0006
2.7921	.0241	7.3548	1.2128	11.9175	.9398	16.4802	1.0199	21.0429	.9949	25.6056	1.0010
2.8602	.0455	7.4229	1.1891	11.9856	.9419	16.5483	1.0201	21.1110	.9944	25.6737	1.0011
2.9283	.0427	7.4910	1.1594	12.0537	.9448	16.6164	1.0196	21.1791	.9942	25.7418	1.0011
2.9964	.0112	7.5591	1.1254	12.1218	.9488	16.6845	1.0184	21.2472	.9943	25.8099	1.0010
3.0645	.0279	7.6272	1.0899	12.1899	.9535	16.7526	1.0168	21.3153	.9945	25.8780	1.0009
3.1326	.0276	7.6953	1.0561	12.2580	.9586	16.8207	1.0153	21.3834	.9946	25.9461	1.0010
3.2007	.0721	7.7634	1.0255	12.3261	.9639	16.8888	1.0139	21.4515	.9946	26.0142	1.0012
3.2688	.3212	7.8315	.9982	12.3942	.9695	16.9569	1.0128	21.5196	.9945	26.0823	1.0014
3.3369	.7356	7.8996	.9726	12.4623	.9759	17.0250	1.0115	21.5877	.9946	26.1504	1.0015
3.4050	1.2831	7.9677	.9470	12.5304	.9838	17.0931	1.0099	21.6558	.9945	26.2185	1.0015
3.4731	1.8857	8.0358	.9206	12.5985	.9931	17.1612	1.0078	21.7239	.9955	26.2866	1.0013
3.5412	2.4408	8.1039	.8942	12.6666	1.0033	17.2293	1.0054	21.7920	.9963	26.3547	1.0009
3.6093	2.8510	8.1720	.8698	12.7347	1.0135	17.2974	1.0028	21.8601	.9971	26.4228	1.0006
3.6774	3.0542	8.2401	.8499	12.8028	1.0225	17.3655	1.0005	21.9282	.9977	26.4909	1.0005
3.7455	3.0403	8.3082	.8360	12.8709	.9295	17.4336	.9986	21.9963	.9982	26.5590	1.0005
3.8136	2.8497	8.3763	.8280	12.9390	1.0345	17.5017	.9970	22.0644	.9986	26.6271	1.0005
3.8817	2.5549	8.4444	.8247	13.0071	1.0380	17.5698	.9956	22.1325	.9990	26.6952	1.0005
3.9498	2.2343	8.5125	.8244	13.0752	1.0408	17.6379	.9941	22.2006	.9996	26.7633	1.0003
4.0179	1.9474	8.5806	.8259	13.1433	1.0432	17.7060	.9924	22.2687	1.0004	26.8314	.9998
4.0860	1.7218	8.6487	.8293	13.2114	1.0453	17.7741	.9907	22.3368	1.0012	26.8995	.9994
4.1541	1.5545	8.7168	.8355	13.2795	1.0466	17.8422	.9891	22.4049	1.0020	26.9676	.9990
4.2222	1.4240	8.7849	.8452	13.3476	1.0464	17.9103	.9880	22.4730	1.0025	27.0357	.9988
4.2903	1.3059	8.8530	.8590	13.4157	1.0445	17.9784	.9875	22.5411	1.0028	27.1038	.9989
4.3584	1.1856	8.9211	.8757	13.4838	1.0410	18.0465	.9875	22.6092	1.0029	27.1719	.9991
4.4265	1.0624	8.9892	.8937	13.5519	1.0368	18.1146	.9877	22.6773	1.0030	27.2400	.9994
4.4946	.9458	9.0573	.9113	13.6200	1.0325	18.1827	.9878	22.7454	1.0032		
4.5627	.8471	9.1254	.9276	13.6881	1.0289	18.2508	.9879	22.8135	1.0035		

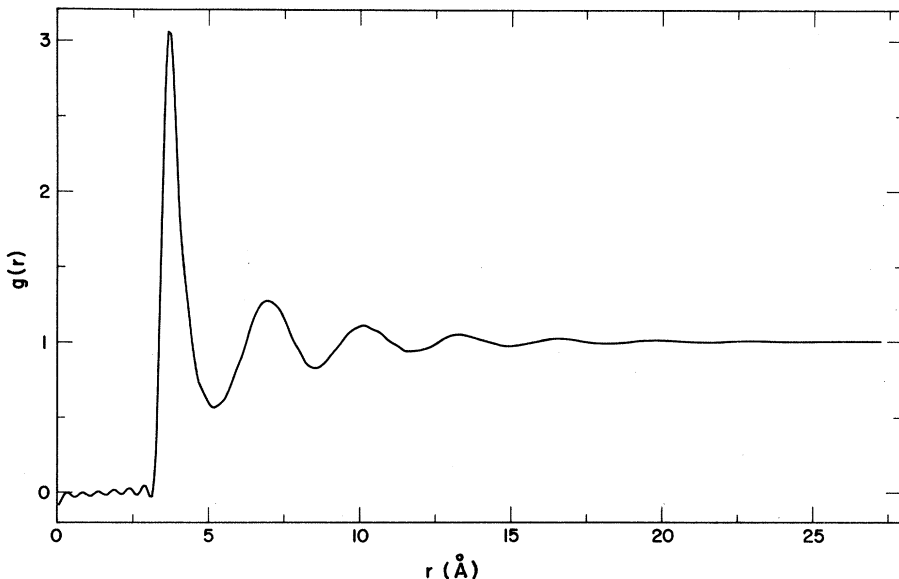


FIG. 4. Radial distribution function $g(r)$ for ^{36}Ar at 85 °K. This curve is the Fourier transform of the smoothed and extended $S(Q)$ shown as a solid line in Fig. 3.

and is listed in Table II. The deviations of the data from the smoothed $S(Q)$ are indicated on an enlarged scale in Fig. 5(a); the rms deviation is computed to be 0.019, which is close to the statistical spread in the data. The iterations may be continued; but it is seen here that for the present data, only one iteration is necessary to yield a smoothed $S(Q)$ which represents the experimental values of $S(Q)$ exceedingly well over the range of Q for which they were measured, and which transforms into a $g(r)$ with satisfactory behavior at small r and for which the spurious residual oscillations have a relatively small amplitude.

V. DISCUSSION

In Fig. 6 the fully corrected data points for $S(Q)$ and the results obtained from molecular-dynamics calculations by Verlet are compared. No adjustments to the data have been made to improve the fit: all corrections and refinements were completed before Verlet's results were received.

The agreement of the data and computations is excellent. Except for a slight difference in the heights of the first peak, where the molecular dynamics results are least accurate and where an error in the calculations of 0.05 or possibly 0.1 is not unreasonable,⁶ there is little if any systematic difference between the data and the calculations, as indicated on an enlarged scale in Fig. 5(b). The rms deviation of the data points from the calculations is 0.022, only slightly larger than the rms deviation from the smoothed $S(Q)$, Fig. 5(a).

Verlet's calculation was for 864 classical point particles in a box, with periodic boundary conditions, interacting pair wise via a Lennard-Jones potential with parameters chosen to give a best fit

to the thermodynamic data of Levelt¹⁸ ($\sigma = 3.405 \text{ \AA}$, $\epsilon/k_B = 119.8 \text{ ^\circ K}$). To the extent that three-body interactions and quantum corrections are impor-

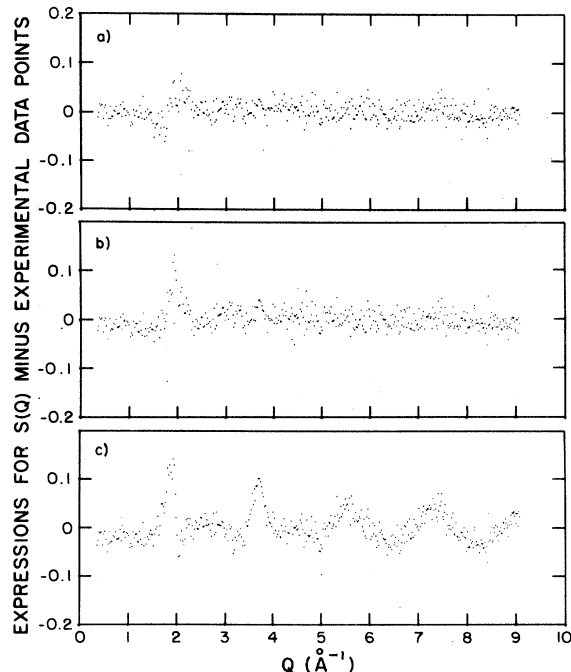


FIG. 5. (a) Deviation of the experimental data from the smoothed and extended $S(Q)$ discussed in the text. (b) Deviation of the experimental data from $S(Q)$ for a Lennard-Jones fluid obtained by Verlet using molecular dynamics. (c) Deviation of the experimental data from $S(Q)$ for a hard-sphere fluid obtained from the Wertheim-Thiele solution of the Percus-Yevick equation. Calculated values of $S(Q)$ corresponding to experimental data points were obtained from tabulated values by spline interpolation.

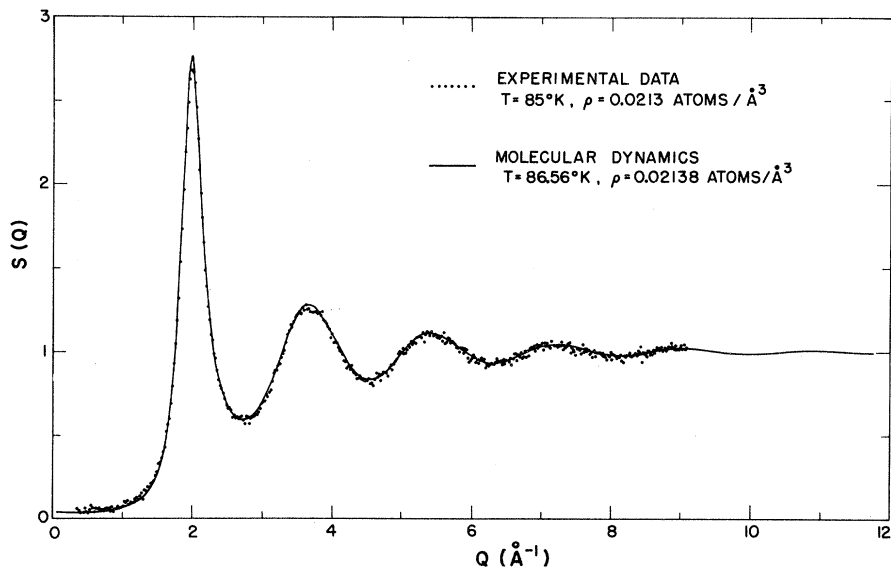


FIG. 6. A comparison of the fully corrected experimental values of $S(Q)$ for liquid argon at 85 °K with $S(Q)$ for a Lennard-Jones fluid in essentially the same state, as calculated by Verlet using molecular dynamics. Final values for both the experimental data and the calculations were obtained independently before the comparison was made.

tant, the potential must be regarded as an effective pair potential.

Recently, a very accurate two-body potential for argon has been obtained by Barker, Fisher, and Watts.⁹ Monte Carlo and molecular-dynamics calculations based on this potential, and which include three-body and quantum corrections, give an excellent description of the properties of solid, liquid, and gaseous argon. Barker has made such a Monte Carlo calculation of $g(r)$ for liquid argon for the conditions of the present experiment.⁸ His results for $g(r)$, which are essentially identical to those obtained by Verlet for the Lennard-Jones potential, are compared with the $g(r)$ obtained from the present experiment in Fig. 7. The agreement

is again excellent.

Page¹⁷ has recently reported $S(Q)$ for liquid normal argon at 84.5 °K, as obtained from a neutron scattering experiment. He compares his data with those reported here, and with the earlier neutron and x-ray scattering data. The agreement between his results and ours is very good; the major discrepancy between Page's corrected data and both ours and the results of molecular dynamics is in the region of low Q .

Sköld *et al.*¹⁸ have recently reported an absolute measurement of the Van Hove response function $S(Q, \omega)$ for liquid argon at 85.2 °K. They point out that $S(Q)$ obtained by calculating the zeroth moment of $S(Q, \omega)$ is everywhere within 10% of our present

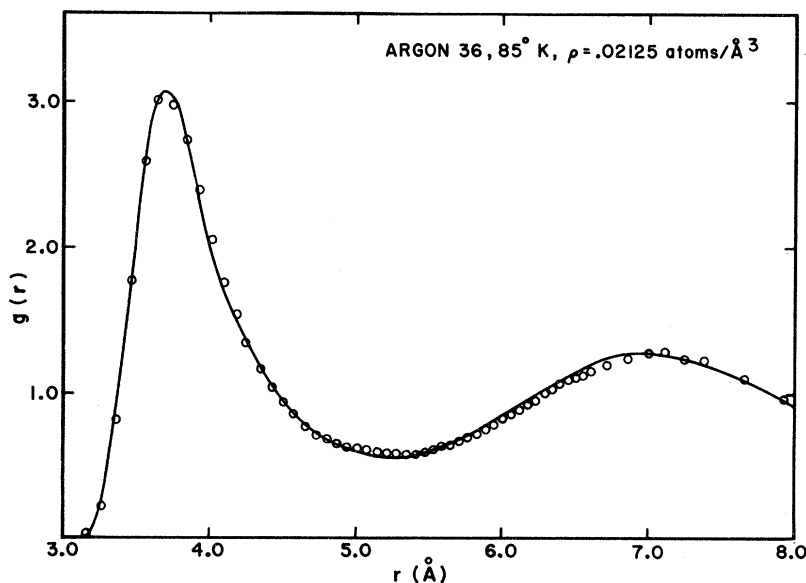


FIG. 7. Comparison of the experimental radial distribution function $g(r)$ (solid curve) and values of $g(r)$ (circles) obtained by Barker from a Monte Carlo calculation based on the potential of Barker, Fisher, and Watts, and including three-body and quantum corrections. The radial distribution function calculated by Verlet using molecular dynamics and the Lennard-Jones potential is indistinguishable from Barker's on the scale of the plot.

results, and "that the agreement, particularly at low Q , is most impressive."

To indicate the degree of sensitivity of $S(Q)$ to the details of the potential, the differences between the corrected data points for $S(Q)$ and the results of a calculation using a hard-sphere interaction potential are shown in Fig. 5(c). The hard-sphere $S(Q)$ was obtained from the Thiele-Wertheim solution of the Percus-Yevick equations,¹⁹ and is for spheres at the same density as in Verlet's calculation. The hard-sphere radius was taken as 1.025σ , which is known to approximate best the calculations for a Lennard-Jones potential.⁷ Though the differences are indeed small and would not be readily apparent on the scale of Fig. 6, they are nonetheless real and systematic. The heights of the peaks are greater for the hard-sphere $S(Q)$, and for larger Q the positions of the peaks shift somewhat. The rms deviation of the data from the hard-sphere $S(Q)$ is 0.033, significantly larger than for the Lennard-Jones case.

In summary, the experimental data and the results of the two computer simulations, which are based on rather different potentials, are all in agreement at a level of ~ 0.01 for $S(Q)$. Calculations based on a hard-sphere potential show small, but significant, deviations from the data. It may be concluded that the structural properties of liquid argon are quite insensitive to the finer details of the potential (or possibly that the Lennard-Jones potential is a rather good effective pair potential). The good agreement with calculations gives assurance that neither the experimental data nor the simulations contain serious errors.

ACKNOWLEDGMENTS

One of us (M.J.K.) would like to express his thanks to Dr. John Yarnell and the Omega West Reactor Group at Los Alamos Scientific Laboratory for their support and hospitality during a post-doctoral appointment. We also thank Dr. S. J. Cocking for the use of his multiple scattering code and his help in applying it, Dr. Loup Verlet for supplying the unpublished molecular-dynamics results for $S(Q)$ used in Fig. 6, and Dr. Daniel Schiff, who together with Verlet, computed the smoothed $S(Q)$, Fig. 3, and $g(r)$, Fig. 4, from our experimental results. Dr. John Barker computed $g(r)$, Fig. 7, at our request, for which we are grateful. Dr. Peter J. Price helped clarify some of Placzek's work and Dr. John Warren extended Placzek's calculations to arbitrary detector efficiency, and contributed constructively to the form of the manuscript.

APPENDIX A: PLACZEK CORRECTIONS

In this Appendix we obtain the relation between $S(Q)$ and the coherent scattering of neutrons by the

liquid, at constant θ , into a detector with an energy-dependent efficiency $\epsilon(k)$. The method is similar to that of Placzek,¹⁵ who treated the case of a $1/v$ detector. It differs from that of Placzek in that an arbitrary $\epsilon(k)$ is assumed, and the Van Hove response function¹¹ $S(Q, \omega)$ is used to describe the properties of the scattering system. In a similar manner we obtain the departure from isotropy of neutrons scattered incoherently by the vanadium calibration standard and by the Ti-Zr cell used in the present experiment.

For the case of coherent scattering by a liquid, the experimental counting rate (after the usual corrections for background, absorption, multiple scattering, etc.) is proportional to an effective differential cross section which is related to $S(Q, \omega)$ by the equation

$$\left(\frac{d\sigma_{coh}}{d\Omega} \right)_{eff} = b_{coh}^2 \int_{-\infty}^{\omega_{max}} \epsilon(k) \left(\frac{k}{k_0} \right) S(Q, \omega) d\omega \quad (A1)$$

with θ constant, where $\hbar\omega_{max}$ is the incident neutron energy E_0 . To obtain $S(Q)$ from the data, the integral at constant θ must be transformed to one at constant Q , Eq. (12). The two integration paths in the $Q-\omega$ plane are shown in Fig. 8, and are represented by the equations:

path I (constant Q),

$$Q_I = 2k_0 \sin \theta ; \quad (A2)$$

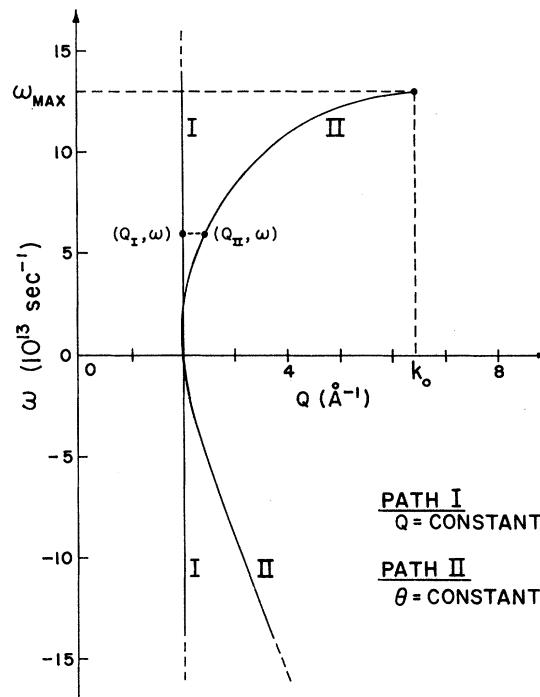


FIG. 8. Integration paths in $Q-\omega$ space. $S(Q)$ is defined by an integral along path I, whereas the experiment measures an integral along path II.

path II (constant θ),

$$Q_{II} = k_0 [2 - \omega/\omega_{max} - 2(1 - \omega/\omega_{max})^{1/2} \cos 2\theta]^{1/2}. \quad (A3)$$

The value chosen for Q_I corresponds to elastic scattering at the angle 2θ . For $\omega=0$, $Q_{II}=Q_I$.

The transformation of the integral is carried out in two steps. First, $S(Q_{II}, \omega)$, a point on path II, is obtained from a Taylor-series expansion of $S(Q, \omega)$ about a point $S(Q_I, \omega)$ on path I, with ω held constant. In this expansion $S(Q, \omega)$ is considered to be a function of Q^2 . Thus

$$\begin{aligned} S(Q_{II}, \omega) &= S(Q_I, \omega) + (Q_{II}^2 - Q_I^2) S'(Q_I, \omega) \\ &\quad + \frac{1}{2}(Q_{II}^2 - Q_I^2)^2 S''(Q_I, \omega) + \dots, \end{aligned} \quad (A4)$$

where the prime indicates differentiation with respect to Q^2 .

The second step is to expand $Q_{II}^2 - Q_I^2$, $\epsilon(k)$, and k/k_0 in powers of $x = \omega/\omega_{max}$ using values of k appropriate for curve II. The required expansions, derivable immediately from Eqs. (1), (2), and (A3), are

$$(Q_{II}^2 - Q_I^2) = -\frac{1}{2}Q_I^2 x + \frac{1}{8}(2k_0^2 - Q_I^2)x^2 + \dots, \quad (A5)$$

$$k/k_0 = 1 - \frac{1}{2}x - \frac{1}{8}x^2 + \dots, \quad (A6)$$

$$\epsilon(k) = \epsilon_0 - \frac{1}{2}k_0\epsilon_1 x + \frac{1}{8}(k_0^2\epsilon_2 - k_0\epsilon_1)x^2 + \dots, \quad (A7)$$

where

$$\epsilon_0 = \epsilon(k_0), \quad \epsilon_1 = \left. \frac{d\epsilon}{dk} \right|_{k=k_0}$$

and

$$\epsilon_2 = \left. \frac{d^2\epsilon}{dk^2} \right|_{k=k_0}.$$

By the use of Eqs. (A4)–(A7), the integrand of (A1) may be expressed as a power series in x in which $S(Q, \omega)$, $\epsilon(k)$, and their derivatives are evaluated at $Q=Q_I$ and $k=k_0$.

Theoretically and experimentally, $S(Q, \omega)$ for any Q is largest near $\omega=0$ and falls to zero as $|\omega|$ increases. If the experimental parameters are chosen such that ω_{max} is large compared to values of $|\omega|$ for which $S(Q, \omega)$ is significantly different from zero, then only the first few terms of the power series need be retained, and the upper limit of the integral in (A1) may be replaced by $+\infty$.

Apart from constants, the integrand now contains only $S(Q, \omega)$ and its derivatives, evaluated at constant Q and multiplied by various powers of ω . When the integration is carried out term by term and differentiations with respect to Q^2 are brought outside the integrals, the result is a series in the frequency moments of $S(Q, \omega)$, defined by

$$\langle \omega^n \rangle_{coh} = \int_{-\infty}^{+\infty} \omega^n S(Q, \omega) d\omega \quad (A8)$$

with Q constant. If terms through the second order in both the Taylor series and the power series in

x are retained, the following expression is obtained after much algebra:

$$\begin{aligned} \left(\frac{d\sigma_{coh}}{d\Omega} \right)_{eff} &= \epsilon_0 b_{coh}^2 \left\{ \langle \omega^0 \rangle_{coh} \right. \\ &\quad - \left(\frac{\hbar}{2E_0} \right) \left[\left(1 + \frac{k_0\epsilon_1}{\epsilon_0} \right) \langle \omega^1 \rangle_{coh} + Q^2 \langle \omega^1 \rangle'_{coh} \right] \\ &\quad - \left(\frac{\hbar^2}{8E_0^2} \right) \left[\left(1 - \frac{k_0\epsilon_1}{\epsilon_0} - \frac{k_0^2\epsilon_2}{\epsilon_0} \right) \langle \omega^2 \rangle_{coh} \right. \\ &\quad \left. \left. - \left(Q^2 + 2k_0^2 + \frac{2Q^2k_0\epsilon_1}{\epsilon_0} \right) \langle \omega^2 \rangle'_{coh} \right. \right. \\ &\quad \left. \left. - Q^4 \langle \omega^2 \rangle''_{coh} \right] \right\}. \end{aligned} \quad (A9)$$

In the above expression, Q is understood to have the value $Q_I = 2k_0 \sin\theta$.

The analysis used to obtain (A9) may also be applied to the case of incoherent scattering, provided $S(Q, \omega)$ is replaced by the "self" part of the response function $S_s(Q, \omega)$ and the coherent scattering length is replaced by the incoherent scattering length b_{inc} . The coherent moments are to be replaced by the incoherent moments

$$\langle \omega^n \rangle_{inc} = \int_{-\infty}^{+\infty} \omega^n S_s(Q, \omega) d\omega \quad (A10)$$

with Q constant.

Expressions for the first few moments of $S(Q, \omega)$ and $S_s(Q, \omega)$ can be obtained from Placzek's paper. A somewhat simpler derivation based on the Van Hove formalism has been given by Rahman, Singwi, and Sjölander (RSS).²⁰ These authors also give the results of calculating the moments classically, together with expressions for the first-order quantum corrections in terms of the potential energy of the scattering system. De Gennes²¹ gives a derivation of the moments for the case in which both recoil and quantum effects are negligible. For most substances and, in particular, for one with an atomic weight as low as argon, the effects of recoil cannot be neglected. On the other hand, the quantum effects are generally negligible. Indeed, for the moments of orders zero and one, the quantum and classical expressions are identical.

The quantum correction to $\langle \omega^2 \rangle_{inc}$, and the leading term in the quantum correction to $\langle \omega^2 \rangle_{coh}$, represent the amount by which the average kinetic energy per atom exceeds the classical value of $\frac{3}{2}k_B T$ (k_B is Boltzmann's constant; T is the absolute temperature). RSS give a rough estimate of this excess, based on the Debye model for the corresponding solid. For liquid argon at 85 °K, the excess is ~5%. We assume the quantum corrections to be negligible in the present application, and drop them in the following analysis. The classical expressions for the moments, including recoil, are

$$\langle \omega^0 \rangle_{coh} = S(Q), \quad \langle \omega^0 \rangle_{inc} = 1,$$

$$\begin{aligned}\hbar\langle\omega^1\rangle_{coh} &= \hbar\langle\omega^1\rangle_{inc} = E_{rec}, \\ \hbar^2\langle\omega^2\rangle_{coh} &= \hbar^2\langle\omega^2\rangle_{inc} = (E_{rec})^2 + 2k_B T E_{rec},\end{aligned}\quad (A11)$$

where $E_{rec} = \hbar^2 Q^2 / 2M$, and M is the mass of an atom in the scattering system.

Classically, E_{rec} is the recoil energy resulting from the transfer of momentum $\hbar\vec{Q}$ to a free atom at rest. The term proportional to $k_B T$ in the second moment results from the Doppler effect. In the present approximation the first and second moments are the same as those of an ideal gas of noninteracting particles, having the same atomic weight and temperature as the scattering system. The influence of the potential is to be found in the spatial correlations which give rise to $S(Q)$, and in the quantum corrections and higher moments.

Substitution of (A11) into (A9) yields

$$\begin{aligned}(\epsilon_0 b_{coh}^2)^{-1} \left(\frac{d\sigma_{coh}}{d\Omega} \right)_{eff} &= S(Q) - C_1 \left(\frac{E_{rec}}{E_0} \right) + C_2 \left(\frac{E_{rec}}{E_0} \right)^2 \\ &- C_3 \left(\frac{E_{rec}}{E_0} \right) \left(\frac{k_B T}{E_0} \right) + \frac{m}{2M} \left(\frac{E_{rec}}{E_0} + \frac{k_B T}{E_0} \right),\end{aligned}\quad (A12)$$

where

$$\begin{aligned}C_1 &= (1 + k_0 \epsilon_1 / 2\epsilon_0), \\ C_2 &= \frac{3}{8} + \frac{5}{4} k_0 \epsilon_1 / 2\epsilon_0 + \frac{1}{4} k_0^2 \epsilon_2 / 2\epsilon_0, \\ C_3 &= -(\frac{3}{2} k_0 \epsilon_1 / 2\epsilon_0 + \frac{1}{2} k_0^2 \epsilon_2 / 2\epsilon_0).\end{aligned}$$

The constants C_i depend on the detector efficiency $\epsilon(k)$. The definitions are such as to make the C_i positive for most detectors. For the detector used in the present experiment,

$$\epsilon(k) = 1 - e^{-1.30k_0/k}. \quad (A13)$$

Table III gives the constants of Eq. (A12) for the above detector, together with values appropriate for $1/v$ and black detectors, illustrating the importance of proper treatment of the detector efficiency in evaluating the Placzek corrections.

In Eq. (A12) the correction term proportional to C_1 comes from the first moment and represents the first-order effect of recoil. The remaining correction terms come from the second moment. Those proportional to $(k_B T / E_0)$ are due to the classical Doppler effect, and the remainder are the second-order effects of recoil. The relative mag-

TABLE III. Dependence of the constants of Eq. (A12) on detector efficiency.

Detector efficiency	$k_0 \epsilon_1 / 2\epsilon_0$	$k_0^2 \epsilon_2 / 2\epsilon_0$	C_1	C_2	C_3
$1/v$	$-\frac{1}{2}^*$	1	$\frac{1}{2}$	0	$\frac{1}{4}$
Eq. (A13)	-0.243	0.170	0.757	0.113	0.280
black	0	0	1	$\frac{3}{8}$	0

nitudes of the correction terms depend on the ratios (E_{rec}/E_0) and $(k_B T/E_0)$.

For the conditions of the present experiment (E_{rec}/E_0) varies between ~ 0 and 0.056, and $(k_B T/E_0) = 0.086$. The correction terms due to the second-order effects of recoil were dropped, yielding the following expressions, which were used to analyze the experimental data:

$$(\epsilon_0 b_{coh}^2)^{-1} \left(\frac{d\sigma_{coh}}{d\Omega} \right)_{eff} = S(Q) + A - B \left(\frac{Q}{k_0} \right)^2, \quad (A14)$$

$$(\epsilon_0 b_{inc}^2)^{-1} \left(\frac{d\sigma_{inc}}{d\Omega} \right)_{eff} = 1 + A - B \left(\frac{Q}{k_0} \right)^2, \quad (A15)$$

where

$$A = (m/2M)(k_B T/E_0),$$

$$B = (m/M)[C_1 + C_3(k_B T/E_0)].$$

For liquid ^{36}Ar under the conditions of the present experiment, $A = 0.0012$ and $B = 0.0219$. The total correction varies from $+0.0012$ at $Q = 0$ to -0.0426 at $Q = 9.08 \text{ \AA}^{-1}$.

It has been contended by Ascarelli and Cagliati²² that the Placzek treatment of the corrections may lead to significant errors. Their procedure was to assume a plausible analytic form for $S(Q, \omega)$ and then perform an expansion to express the effective cross section as the sum of $S(Q)$ and several correction terms. To represent $S(Q, \omega)$ they used the product of $S(Q)$ and a Gaussian in ω chosen to yield the De Gennes expression for the second moment. The correction terms depend on the slope and curvature of $S(Q)$, and the authors conclude that certain of the correction terms are important, especially where the curvature of $S(Q)$ is high.

The expressions given by Ascarelli and Cagliati are inappropriate for the present experiment for two reasons: First, they completely neglect recoil, which is the largest effect for the case of liquid argon; second, they assume a black detector. Nevertheless, a similar approach may be used to estimate the accuracy of the Placzek procedure as we have used it.

Following Ascarelli and Cagliati, we approximated $S(Q, \omega)$ by the product of $S(Q)$ and a Gaussian in ω chosen to yield the classical values, including recoil, for both the first and second moments [Eq. (A11)]. The molecular-dynamics calculations of Verlet⁷ were used for $S(Q)$. A contour plot of this $S(Q, \omega)$ is shown in Fig. 9, together with several curves of constant θ , for the conditions of the present experiment. The integral for the effective cross section, Eq. (A1), was carried out numerically using this $S(Q, \omega)$. Equation (A13) was used for the detector efficiency. The Placzek correction, Eq. (A14), was then applied. The resulting "experimental" values of $S(Q)$ were compared with

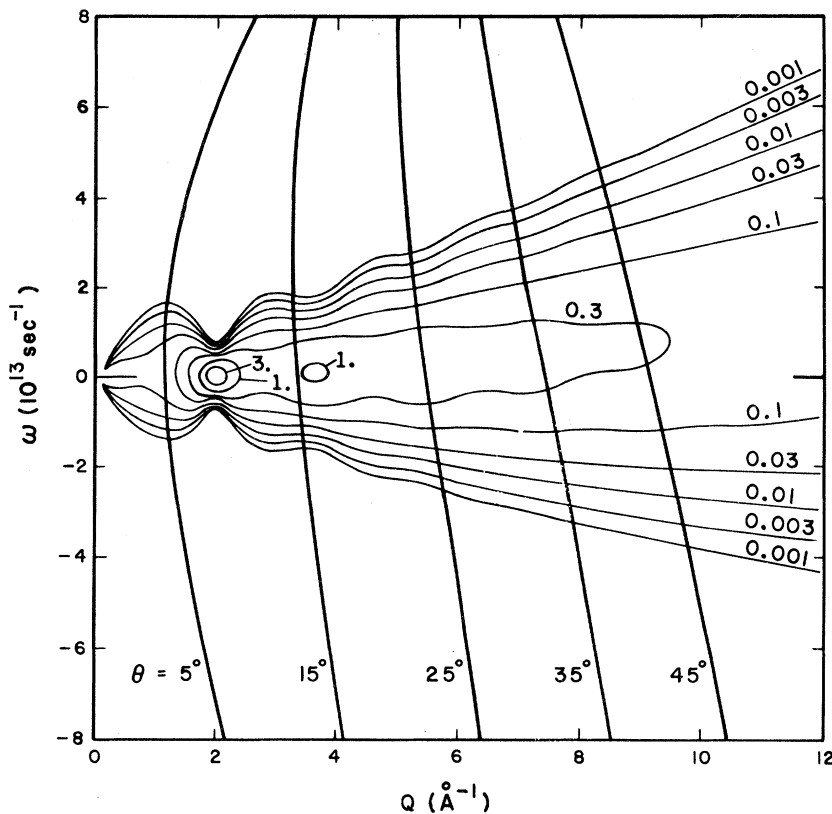


FIG. 9. Logarithmic contour plot of a Gaussian approximation to $S(Q, \omega)$ for liquid ^{36}Ar at 85 °K chosen to have the correct classical first and second moments of ω . Also shown are curves of constant θ for the conditions of the present experiment.

the molecular-dynamics $S(Q)$ originally assumed. The difference is shown as a function of Q in Fig. 10. For $Q \leq 6 \text{ \AA}^{-1}$ the deviations are < 0.001 , while for $Q \leq 9 \text{ \AA}^{-1}$ the maximum deviation is 0.0022. Since the level of accuracy in the present experiment is ~ 0.01 , the Placzek procedure is clearly adequate.

APPENDIX B: OTHER CORRECTIONS

In addition to the Placzek corrections described in Appendix A, several other corrections must be applied to the raw data to obtain $S(Q)$ on an absolute basis. These corrections are discussed below.

The effects of instrumental resolution were

negligible except in the region of the first peak in the argon data. For this region a resolution correction was made by the method of Jones and Misell.²³ To apply this method, analytic representations of both the resolution function and the observed data are required. The spectrometer resolution was well represented by a Gaussian in θ , and the data in the region of the first peak could be fitted by a Gaussian plus a second-degree polynomial. Using these representations, a resolution correction was calculated and applied to the individual data points. The maximum correction was 1.7%.

After the resolution correction had been applied,

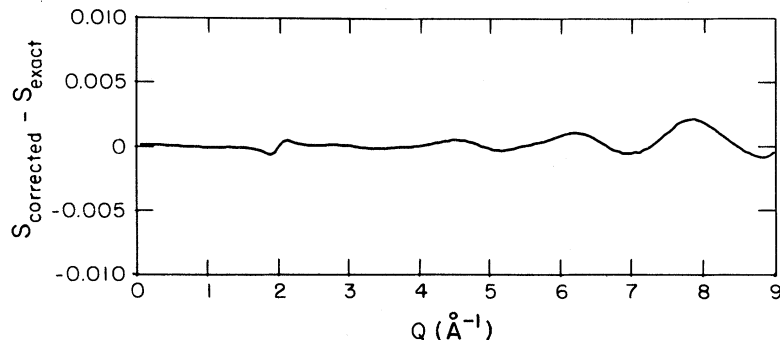


FIG. 10. Deviation of the corrected "experimental" $S(Q)$ from the assumed exact $S(Q)$ as calculated numerically for the Gaussian approximation to $S(Q, \omega)$ shown in Fig. 9. This deviation is a realistic estimate of the uncertainties in $S(Q)$ resulting from use of the Placzek procedure.

the background was subtracted and corrections were made for transmission and variation of the amount of scattering material in the beam. Since the incident neutron beam fell within the uniform central portion of the flat Ti-Zr cell at all scattering angles, and the normal to the cell bisected the scattering angle, both the path length of neutrons in the cell and sample and the volume of cell and sample material in the beam are proportional to $\sec\theta$ (see Fig. 1). One may readily derive

$$J_s(\theta) = \frac{\cos\theta}{fT_{C+S}^{\sec\theta}} [I_{C+S} - fI_C T_S^{\sec\theta} - (1-f)I_C], \quad (B1)$$

where $J_s(\theta)$ is the corrected scattering intensity from the sample and I is the observed intensity. Here, the subscripts C and S are for cell and sample, respectively, f is the fraction of the cell occupied by sample, and T is the transmission for $\theta=0$. Note that for the fraction of the cell occupied by the sample, the amount of background scattering to be subtracted must be reduced by the transmission of the sample. For purposes of calibration, the corrected scattering intensity from the vanadium standard J_v and from the Ti-Zr cell J_c were also calculated using formulas similar to (B1).

In addition to the desired intensity of single scattering, J_s contains contributions from multiple scattering in the cell and sample material. By subtracting the background, those multiple scattering events which take place exclusively in the cell material have been removed. There remain those events which take place in the sample together with those events which involve both materials. Thus the effective multiple scattering contribution is given by

$$M_{\text{eff}}(\theta) = M_{C+S}(\theta) - M_C(\theta), \quad (B2)$$

where the subscripts C and S again represent the cell and sample. The method of Cocking and Heard²⁴ was used to calculate $M_{\text{eff}}(\theta)$ at 1° intervals in θ , and the value to be used at each scattering angle was obtained by interpolation.

In Cocking and Heard's method the twice-scattered component is calculated explicitly, using the angular distribution of single scattering which is presumed known. The higher components are estimated. In making the calculations expressions (A14) and (A15) were used for the angular distributions. Verlet's molecular-dynamics calculations were used to estimate $S(Q)$. Identical results were obtained when an approximate experimental value was used for $S(Q)$. The cell plus sample and the empty cell were treated as uniform distributions of scattering material with appropriately averaged cross sections. The resulting multiple scattering contribution was isotropic within 1.8% in the range $1^\circ \leq \theta \leq 45^\circ$ with an average value of 0.381. This may be understood by noting that the impor-

tant events are those in which the first scattering lies in the plane of the sample. For these events, the scattering angles are large and the cross section is relatively constant.

Geometric factors and detector efficiencies were combined to give an over-all spectrometer sensitivity $F(\theta)$ which was allowed to depend on the scattering angle θ to account for possible imperfections in alignment. The corrected scattering intensity from the vanadium standard $J_v(\theta)$ was used to determine $F(\theta)$ from the relation

$$J_v(\theta) = \rho\sigma_v t F(\theta) [1 + A - B(Q/k_0)^2 + M_v(\theta)], \quad (B3)$$

where ρ is the number of target atoms per unit volume, σ_v is the bound-atom incoherent scattering cross section of vanadium (5.10 ± 0.02 b),²⁵ and t is the target thickness. The terms A and B are Placzek corrections defined in Appendix A and $M_v(\theta)$ is the multiple scattering contribution discussed above.

The (110) and (211) Bragg peaks were clearly visible above the incoherent background in J_v . Points in the neighborhood of these peaks were discarded and the remaining points were used to obtain $F(\theta)$. The experimentally determined $F(\theta)$ was well represented by a constant plus a term linear in θ . The linear term was negative, and amounted to 1.8% of the constant term at the largest scattering angle.

As a check of the calibration procedures, a reduced angular distribution $X(Q)$ was calculated for the Ti-Zr cell from the relation

$$X(Q) = [\rho\sigma_c t F(\theta)]^{-1} J_c(\theta) - A + B(Q/k_0)^2 - M_c(\theta). \quad (B4)$$

If the Ti-Zr cell material is truly a random alloy and if the corrections and cross sections used are correct, $X(Q)$ should be unity, independent of Q . The experimental $X(Q)$ could be described as a constant plus a variable term reminiscent of $S(Q)$ for a liquid. The latter term was ~10% of the former. We attribute it to the presence of short-range order in the Ti-Zr alloy. This effect has been seen in several samples of the alloy. The asymptotic value of $X(Q)$ at large Q was 0.97 rather than 1.00 as expected. The discrepancy is probably due to uncertainties in the cross sections and in the multiple scattering contribution, and is indicative of the accuracy we can expect in the determination of $S(Q)$ for liquid argon on an absolute basis. The relative error in the experimental $S(Q)$ for different values of Q is expected to be much less than the absolute error.

In addition to neutrons of wave number k_0 , the incident neutron beam contained a second-order component of wave number $2k_0$. At each scattering angle, therefore, one observes a superposition of contributions from $S(Q)$ and $S(2Q)$. If p is the effective fraction of the neutron beam of wave num-

ber k_0 , then

$$[\rho\sigma_S tF(\theta)]^{-1}J_S(\theta) = pS_{\text{eff}}(Q) + (1-p)S_{\text{eff}}(2Q) + M_{\text{eff}}(\theta), \quad (\text{B5})$$

where $S_{\text{eff}} = S$ plus the appropriate Placzek terms. Equivalent values of $S(2Q)$ were obtained from approximate experimental data and from molecular-dynamics calculations. The errors introduced in the multiple scattering calculation by assuming all the incident neutrons to be first order are considered to be negligible.

The effective fraction p of first-order neutrons in the incident beam was determined to be 0.987 from an analysis of the weak second-order peaks visible in the standard powder diffraction pattern used to determine the incident neutron wavelength.

The effect of the second-order neutrons may be seen as a small anomaly at $\theta = \sim 4.5^\circ$ in the raw cell-plus-sample data shown in Fig. 2.

Equation (B5) may be solved for $S(Q)$, yielding

$$\begin{aligned} S(Q) = (1/p) & \{ [\rho\sigma_S tF(\theta)]^{-1}J_S(\theta) - A + B(Q/k_0)^2 \\ & - (1-p)S_{\text{eff}}(2Q) - M_{\text{eff}}(\theta) \}. \end{aligned} \quad (\text{B6})$$

Expression (B6) was taken as the best estimate of the absolute value of $S(Q)$ for liquid argon.

APPENDIX C: REFINEMENT OF $S(Q)$

As indicated in Appendix B the experimental data

yield $S(Q)$ with an absolute error of the order of 0.03. The principal sources of error are believed to be in the assumed cross sections and multiple scattering corrections, which are essentially independent of Q . Thus the experimental results can be improved by adjusting the cross section and the multiple scattering contribution so that the experimental $S(Q)$ satisfies the integral relationships stated in Sec. II, Eqs. (9) and (10). These normalization relationships ensure that both $S(Q)$ and its Fourier transform $g(r)$ have the correct limiting values as their arguments approach zero. The net correction amounted to an adjustment to the computed multiple scattering correction by 0.021, and a scaling of $S(Q)$ by about 2%.

In carrying out the adjustment, it is necessary to extrapolate the experimental data to $Q=0$. The statistical spread in the low- Q data is too great to permit a detailed determination of the functional form of $S(Q)$ in this region, which might be used as a guide in making the extrapolation. Since the experimental $S(Q)$ is relatively constant in the range $0.35 \text{ \AA}^{-1} \leq Q \leq 0.75 \text{ \AA}^{-1}$, we have chosen to take the average of the experimental data in this region to be the extrapolated value of $S(Q)$ at $Q=0$. The compressibility limit for $S(Q)$, Eq. 9, was taken to be 0.0522, based on an isothermal compressibility¹⁴ of $2.12 \times 10^{-4} \text{ atm}^{-1}$.

¹Work supported by the U. S. Atomic Energy Commission.

²L. Verlet, Phys. Rev. 165, 201 (1968).

³D. Levesque and L. Verlet, Phys. Rev. Letters 20, 905 (1968).

⁴P. G. Mikolaj and C. J. Pings, J. Chem. Phys. 46, 1401 (1967); J. Chem. Phys. 46, 1412 (1967).

⁵V. E. Krohn and G. R. Ringo, Phys. Rev. 148, 1303 (1966).

⁶D. M. North, J. E. Enderby, and P. A. Egelstaff, Pro. Phys. Soc. London, 1, 784 (1968).

⁷L. Verlet and D. Schiff (private communications).

⁸L. Verlet, Phys. Rev. 165, 201 (1967); and private communication.

⁹J. Barker (private communication).

¹⁰J. A. Barker, R. A. Fisher, and R. O. Watts, Mol. Phys. 21, 657 (1971).

¹¹P. A. Egelstaff, *An Introduction to the Liquid State* (Academic, London, 1967), pp. 21–22.

¹²L. Van Hove, Phys. Rev. 95, 249 (1954).

¹³S. S. Sidhu, L. Heaton, D. D. Zauberes, and F. P. Campos, J. Appl. Phys. 27, 1040 (1956).

¹⁴C. Kempter (private communication).

¹⁵P. J. Hunter and J. S. Rowlinson, in *Simple Dense Fluids*, edited by H. L. Frisch and Z. W. Salsberg (Academic, New York, 1968).

¹⁶G. Placzek, Phys. Rev. 86, 377 (1952).

¹⁷J. M. H. Levelt, Physica 26, 361 (1960).

¹⁸D. I. Page, Harwell Report No. AERE-R6828, 1972 (unpublished).

¹⁹K. Sköld, J. M. Rowe, G. Ostrowski, and P. D. Randolph, Phys. Rev. A 6, 1107 (1972).

²⁰E. J. Thiele, J. Chem. Phys. 38, 1959 (1963); M. S. Wertheim, Phys. Rev. Letters 10, 321 (1963).

²¹A. Rahman, K. S. Singwi, and A. Sjölander, Phys. Rev. 126, 986 (1962). These authors differ formally from Placzek in their expression for the interference contribution to $\langle \omega^2 \rangle_{\text{coh}}$ owing to a different choice for the order of noncommuting operators in a quantum statistical average. By considering the commutation relations, the two expressions for the interference contribution can be shown to be the same.

²²P. De Gennes, Physica 25, 825 (1959). De Gennes's definitions of the moments differ from ours in that his higher moments are normalized by dividing by the corresponding moment of order zero.

²³P. Ascarelli and G. Caglioti, Nuovo Cimento 43B, 376 (1966).

²⁴A. F. Jones and C. L. Misell, Brit. J. Appl. Phys. 18, 1479 (1967).

²⁵S. J. Cocking and C. R. T. Heard, Harwell Report No. AERE-R5016, 1965 (unpublished).

²⁶D. J. Hughes and Robert B. Schwartz, Brookhaven Report No. BNL-325, 2nd ed., 1958 (unpublished).